EPJ Web of Conferences **119**, 15006 (2016) DOI: 10.1051/epjconf/201611915006
*ILRC 27*

# ATMOSPHERIC BOUNDARY LAYER HEIGHT EVOLUTION WITH LIDAR IN BUENOS AIRES FROM 2008 TO 2011

**Ezequiel Eduardo Pawelko[1], Jacobo Omar Salvador[1], Pablo Roberto Ristori[1], Juan Vicente Pallotta[1], Lidia Ana Otero[1], Eduardo Jaime Quel[1]**

[1] *CEILAP (CITEDEF-CONICET), UMI-IFAECI-CNRS 3351, Juan B. de La Salle 4397, B1603ALO, Villa Martelli, Buenos Aires, Argentina, E-mail: epawelko@citedef.gob.ar*

**ABSTRACT**

The analysis of the atmospheric boundary layer top height evolution is obtained from 2008 to 2011 in Buenos Aires using the multiwavelength lidar located at CEILAP (CITEDEF-CONICET) (34°33' S; 58°30' W; 17 m asl). Algorithms recognition based on covariance wavelet transform are applied to obtain seasonal statistics. This method is being evaluated for use in the Lidar Network in Argentina and it is being deployed in Patagonia region currently. The technique operates in real time in both low and high aerosol loads and with almost no human supervision.

## 1. INTRODUCTION

The Atmospheric Boundary Layer (ABL) is the lowest layer that is directly influenced by the Earth´s surface. It responds to surface forcing by frictional drag, evaporation and transpiration, and sensible heat transfer with a timescale of one hour or less [1]. Lidar, light detection and ranging, is a valuable tool to study the atmospheric boundary layer. This instrument works with high spectral and spatial resolution that allows identifying the ABL height. Aerosol vertical structure is considered as a good tracer to determine the ABL height. Lidar backscatter profiles show a strong negative gradient at the top of this layer which can be recognized with different mathematic methods. Algorithms based on threshold values [2], minimum vertical gradient in the lidar profile [3], maximum in variances of signals [4] and a method that fits an idealized profile [5] are widely used. It is recognized that these approaches are sensitive to noise and small-scale structure in the lidar profiles.

A robust algorithm based on CWT (Covariance Wavelet Transform) is proposed by [6, 7]. The method can recognize the ABL height in profiles with lower signal to noise ratio than other algorithms.

## 2. METHOD AND RESULTS

### 2.a. Lidar setup

The tropospheric multiwavelength lidar system was developed to monitor range-resolved aerosol optical properties. Its dynamic range covers a region from 200 m to 10 km in coaxial overlap (from 2009 up to present) and from 600 m to 10 km in biaxial overlap setup. The lidar emission system is based on a Nd:YAG laser (Continuum Surelite III P-IV) with 3 wavelengths at 10 Hz (650 mJ at 1064 nm). First and second harmonic are also generated. The IR wavelength is normally used for studying the ABL. The backscattered radiation is collected by an f/2, 1 m focal length Newtonian telescope and focused into a 1.8 mm diameter optical fiber that works as a field stop. The data acquisition system had a 20 MHz sampling rate and a 7.5 m vertical resolution [8].

### 2.b.- Method

The ABL height recognition is obtained applying a CWT (Covariance Wavelet Transform) and Haar function based algorithm [7]. CWT and Haar function are shown in equations 1 and 2 respectively. In those part, $a$ and $b$ are the dilatation and translation factors respectively, $z$ is the height vector and $f(z)$ is the lidar profile. The atmospheric boundary layer height is presented as an abrupt decrease of the lidar backscatter.

$$W_f(a,b) = \frac{1}{a}\int_{z_1}^{z_2} f(z)\,h\left(\frac{z-b}{a}\right)dz \tag{1}$$

$$h\left(\frac{z-b}{a}\right) = \begin{cases} +1: \ b-a/2 \le z \le b \\ -1: \ b \le z \le b+a/2 \\ \ \ 0: \ \text{elsewhere} \end{cases} \tag{2}$$

Equation 3 is the spectral variance proposed by [7, 9] to calculate the wavelet dilation factor. The traslation $b$ that produces the maximum value in CWT is the atmospheric boundary layer top height.

DOI: 10.1051/epjconf/201611915006

$$\left[ D^2(a) = \int_{z_1}^{z_2} \left[ W_f(a,b) \right]^2 db \right]_{Max} = a \qquad (3)$$

**2.c.- Results**

The results of a seasonal study of the ABL height evolution with lidar between 2008 and 2011 are presented. 197 days of measurements are processed. The ABL height is obtained from 1064 nm backscatter wavelength. Measurements with clouds supported on the ABL are not processed.

Figures 1 to 4 show the ABL height evolution in the summer, fall, winter and spring.

(a)

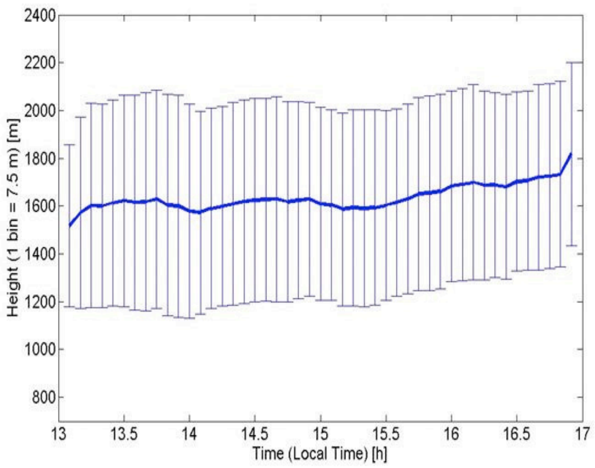


(b)

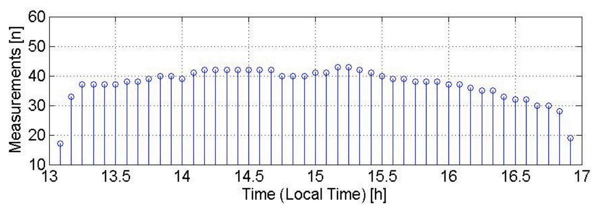


*Figure 1. (a) Daytime ABL height evolution (mean value +- one standard deviation) in the summer between 2008 and 2011 (1064 nm, 7.5 m spatial resolution, 5 min temporal resolution) (50 measurements: 03/1/2008, 03/25/2008, 01/05/2009, 01/09/2009, 01/20/2009, 01/21/2009, 01/22/2009, 01/23/2009, 01/26/2009, 02/02/2009, 02/06/2009, 02/12/2009, 02/17/2009, 02/18/2009, 02/19/2009, 02/25/2009, 02/26/2009, 12/30/2009, 01/05/2010, 01/08/2010, 01/12/2010, 01/13/2010, 01/21/2010, 01/22/2010, 01/24/2010, 01/25/2010, 01/28/2010, 01/29/2010, 02/08/2010, 02/11/2010, 02/12/2010, 03/15/2010, 03/16/2010, 12/21/2010, 12/27/2010, 01/06/2011, 01/18/2011, 01/20/2011, 01/21/2011, 02/02/2011, 02/03/2011, 02/04/2011, 02/14/2011, 02/15/2011, 03/01/2011, 03/02/2011, 03/14/2011, 03/18/2011, 12/27/2011, 12/29/2011). (b) Number of measurements processed at each time interval.*

(a)

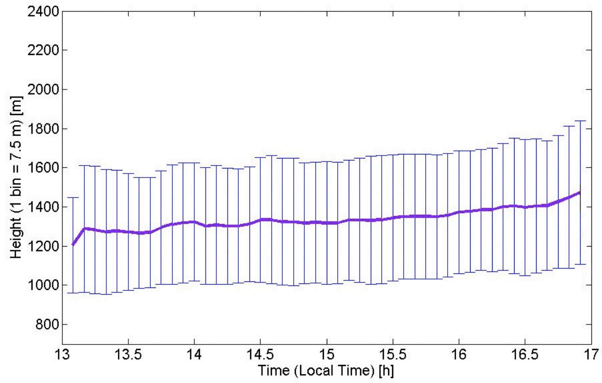


(b)

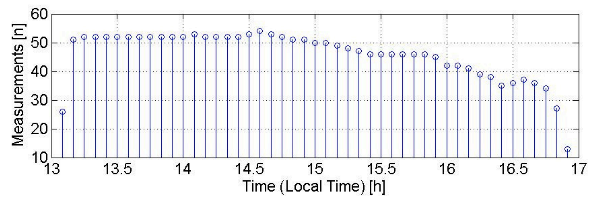


*Figure 2. (a) Daytime ABL height evolution (mean value +- one standard deviation) in the fall between 2008 and 2011 (1064 nm, 7.5 m spatial resolution, 5 min temporal resolution) (57 measurements: 04/08/2008, 04/10/2008, 04/14/2008, 04/17/2008, 04/18/2008, 04/21/2008, 04/22/2008, 04/24/2008, 04/25/2008, 05/01/2008, 05/05/2008, 05/06/2008, 05/09/2008, 05/10/2008, 05/29/2008, 05/30/2008, 06/06/2008, 06/10/2008, 06/12/2008, 06/13/2008, 06/17/2008, 03/23/2010, 03/25/2010, 03/29/2010, 04/05/2010, 04/06/2010, 04/16/2010, 04/22/2010, 04/23/2010, 04/26/2010, 04/28/2010, 04/29/2010, 04/30/2010, 05/07/2010, 05/10/2010, 05/12/2010, 06/01/2010, 06/07/2010, 03/21/2011, 03/28/2011, 03/30/2011, 04/01/2011, 04/06/2011, 04/26/2011, 04/27/2011, 05/02/2011, 05/03/2011, 05/04/2011, 05/06/2011, 05/09/2011, 05/19/2011, 06/07/2011, 06/08/2011, 06/09/2011, 06/10/2011, 06/13/2011, 06/14/2011). (b) Number of measurements processed at each time interval.*

(a)

DOI: 10.1051/epjconf/201611915006

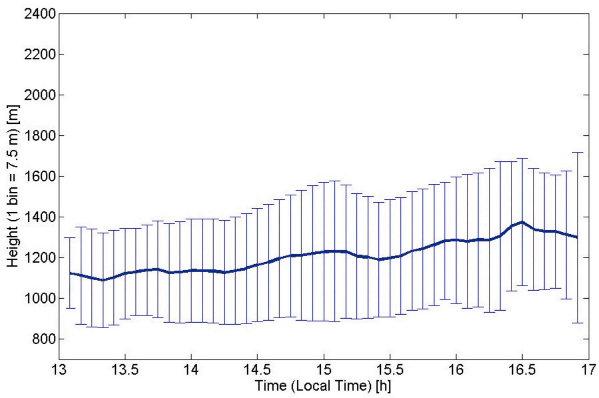


(b)

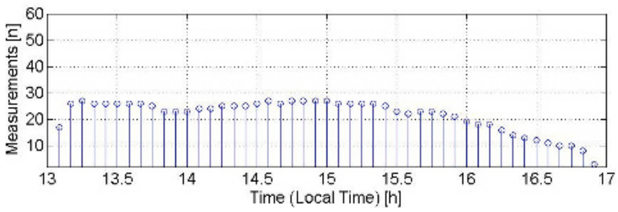


*Figure 3. (a) Daytime ABL height evolution (mean value +- one standard deviation) in the winter between 2008 and 2011 (1064 nm, 7.5 m spatial resolution, 5 min temporal resolution)(38 measurements: 09/12/2008, 09/17/2008, 08/11/2009, 08/20/2009, 08/26/2009, 09/09/2009, 06/28/2010, 07/15/2010, 07/16/2010, 07/23/2010, 08/092010/, 08/20/2010, 08/24/2010, 08/25/2010, 09/06/2010, 09/07/2010, 09/09/2010, 09/14/2010, 06/27/2011, 06/28/2011, 06/29/2011, 07/01/2011, 07/02/2011, 07/06/2011, 07/12/2011, 07/28/2011, 07/29/2011, 08/03/2011, 08/04/2011, 08/05/2011, 08/11/2011, 08/23/2011, 08/25/2011, 08/30/2011, 09/02/2011, 09/12/2011, 09/14/2011, 06/29/2011). (b) Number of measurements processed at each time interval.*

(a)

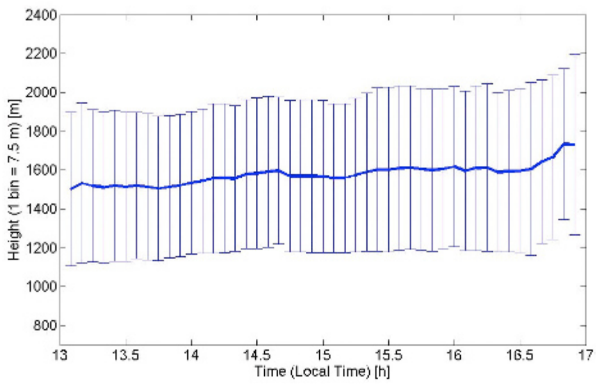


(b)

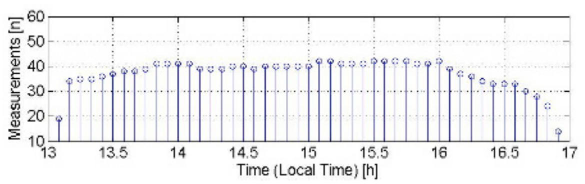


*Figure 4. (a) Daytime ABL height evolution (mean value +- one standard deviation) in the spring between 2008 and 2011(1064 nm, 7.5 m spatial resolution, 5 min temporal resolution)(52 measurements: 09/22/2008, 09/25/2008, 09/26/2008, 10/02/2008, 10/06/2008, 10/16/2008, 10/20/2008, 10/24/2008, 10/29/2008, 10/30/2008, 10/31/2008, 11/05/2008, 11/06/2008, 11/13/2008, 11/17/2008, 11/21/2008, 12/03/2008, 12/04/2008, 12/05/2008, 12/15/2008, 12/16/2008, 11/05/2009, 11/16/2009, 10/04/2010, 10/12/2010, 11/24/2010, 11/29/2010, 12/01/2010, 12/02/2010, 12/03/2010, 12/06/2010, 12/16/2010, 09/27/2011, 10/03/2011, 10/06/2011, 10/11/2011, 10/17/2011, 10/18/2011, 10/20/2011, 10/21/2011, 10/26/2011, 10/27/2011, 10/31/2011, 11/01/2011, 11/11/2011, 11/16/2011, 11/22/2011, 11/23/2011, 11/29/2011, 12/01/2011, 12/07/2011, 12/12/2011). (b) Number of measurements processed at each time interval.*

Table I presents results of ABL height in Buenos Aires.

*Table I. seasonal atmospheric boundary layer height between 2008 and 2011.*

| Seasons | Measurements [n] | ABL top height [m] | |
|---|---|---|---|
| | | Mean | Standard deviation |
| Summer | 50 | 1634.9 | 411.6 |
| Fall | 57 | 1336.5 | 314.6 |
| Winter | 38 | 1208.0 | 285.7 |
| Spring | 52 | 1577.9 | 399.4 |

## 3. CONCLUSIONS

A preliminary seasonal study of the daytime atmospheric boundary layer height evolution is performed with aerosol lidar and an algorithm based on covariance wavelet transform. A database of 197 lidar measurements in Buenos Aires is processed. The results show that this layer varies depending on the season, between 1223 and 2046 m in the summer, 1021 and 1651 m in the fall, 922 and 1493 m in the winter and between 1178 and 1977 m in the spring, using mean value with one standard deviation computed from 13 to 17 h local time.

## ACKNOWLEDGMENTS

Authors would like to thank JICA (Japan International Cooperation Agency) and JST (Japan Science and Technology Agency) through the Science and Technology Research Partnership for Sustainable Development (SATREPS) for supporting this work under the project: "Development of Atmospheric Environmental Risk Management System in South America".

## REFERENCES

[1] Stull R. 1998: "*An Introduction to Boundary Layer Meteorology*", Kluwer Academic Publishers, Dordrecht, Boston, London.

[2] Boers, R., E. Eloranta, 1986: Lidar measurements of the atmospheric entrainment zone and the potential temperature jump across the top of the mixed layer; Bound.-Lay. Meteorol., **34**, pp. 357–375.

[3] Flamant, C., J. Pelon, P. Flamant, P. Durand, 1997: Lidar determination of the entrainment zone thickness at the top of the unstable marine atmospheric boundary layer, Bound.-Lay. Meteorol., **83**, pp. 247–284.

[4] Hooper, W., E. Eloranta, 1986: Lidar measurements of wind in the planetary boundary layer: the method, accuracy and results from joint measurements with radiosonde and kytoon, J. Clim. Appl. Meteor., **25**, pp. 990–1001.

[5] Steyn, D., M. Baldi, R. Hoff, 1999: The detection of mixed layer depth and entrainment zone thickness from lidar backscatter profiles, J. Atmos. Ocean Tech., **16**, pp. 953–959.

[6] Cohn, S., W. Angevine, 2000: Boundary layer height and entrainment zone thickness measured by lidars and wind-profiling radars, J. Appl. Meteor., **39**, pp. 1233–1247

[7] Davis K., N. Gamage, C. Hagelberg, C. Kiemle, D. Lenschow, P. Sullivan, 2000: An objective method for deriving atmospheric structure from airborne lidar observations, J. Atmos. Oceanic. Technol., **17**, pp. 1455-1468.

[8] Otero L., P. Ristori, E. Pawelko, J. Pallotta, E. Quel, 2011: Six-Year Evolution of Multiwavelength Lidar System at CEILAP, V Workshop on Lidar Measurements in Latin America, Opt. Pura Apl., **44**, pp. 13-18.

[9] Gamage N., C. Hagelberg, 1993: Detection and Analysis of Microfronts and Associated Coherent Events Using Localized Transforms. J. Atmos. Sci., 50, pp. 750–756.